Use of a Programmable Monochromator and a SIT Detector in Flame Atomic Emission Spectrometry

Naoki FURUTA,*,† Cameron W. McLEOD,** Hiroki HARAGUCHI,** and Keiichiro FUWA**

Division of Chemistry and Physics, National Institute for Environmental Studies, Yatabe, Ibaraki 300-21

***Department of Chemistry, Faculty of Science, The University of Tokyo, Bunkyo-ku, Tokyo 113*

(Received March 15, 1979)

A multielement detection system which uses a programmable monochromator and a SIT image detector has been constructed, and evaluated by measuring the flame emission of 22 elements in the nitrous oxide–acetylene flame. The detection limits for the elements under optimized experimental conditions are reported, and are compared with those obtained by a standard photomultiplier tube.

The silicon intensified target tube (SIT) coupled with an optical multichannel analyser (OMA) has been utilized as a detector system in emission,[1-6] absorption[7-9] and fluorescence[10] spectroscopic studies. Attractive analytical features of the SIT detection system, which have been well-documented in the reports from Morrison and his coworkers,[1,4-6] include the simultaneous multielement analysis capability, the facility to correct for spectral and background interference and detection power equivalent to the photomultiplier tube (PMT) in the visible region, although detection performance is relatively poorer in the ultraviolet. As is well known,[11] the standard SIT image detector consists of about 500 light sensitive elements (channels) within an area of approximately 62.5 mm^2 (length 12.5 mm, height 5 mm) so that, when situated in a dispersing instrument, simultaneous detection of atomic lines is possible. The range of wavelengths which are detected simultaneously is determined primarily by the reciprocal linear dispersion (RLD) of the monochromator. In order to take advantage of the SIT–OMA system for simultaneous multielement analysis, relatively low-dispersion monochromators which provide a spectral window generally greater than 20 nm have been preferred. The use of the low-dispersion monochromator, however, may result in severe spectral interference in atomic emission spectroscopy in high temperature media, particularly in inductively coupled plasma (ICP) emission spectroscopy.

In the present study, the SIT–OMA system has been combined with a medium resolution monochromator (focal length, 1 m; RLD, 0.4 nm/mm) to evaluate detectability performance. The use of the medium resolution monochromator reduces the spectral region spatially detected by the SIT–OMA system (5 nm for present instrumentation) and sacrifices to some extent the capability for simultaneous multielement analysis.

Recently, the present authors have developed a programmable monochromator controlled by a minicomputer, where a slew-scan technique was employed as has been reported by other workers.[12-16] The programmable monochromator of the slew scan type is convenient for rapid sequential multielement analysis and has more inherent flexibility for multielement detection than the well-established direct reading system where only fixed wavelengths of the desired elements are available.[17] However, the slew scan technique suffers from the problem of irreproducibility in wavelength setting, precision being limited to ± 0.1 nm, as has already been pointed out.[13,16] To avoid the error caused by irreproducible wavelength setting in the slit-based spectrometer, it was decided to adopt the SIT as the spatial detector in the slew scan system. The important capability of simultaneous multielement analysis is still retained provided element lines are within a 5 nm range for the present instrumentation (± 2.5 nm from the central OMA channel).

In this study, the analytical performance of the SIT–OMA-detector is considered when combined with the programmable monochromator system. The nitrous oxide–acetylene flame was selected as the excitation source for initial studies.

Experimental

Instrumentation. The experimental system is shown in Fig. 1. A nitrous oxide†† –acetylene flame was supported on a burner assembly (5 cm slot burner) of a commercially available spectrophotometer (Shimadzu AA 650). The monochromator (Jobin Yvon HR 1000; focal length, 1 m) had dual entrance and exit ports and was equipped with a holographic grating (2400 grooves/mm); the desired optical path

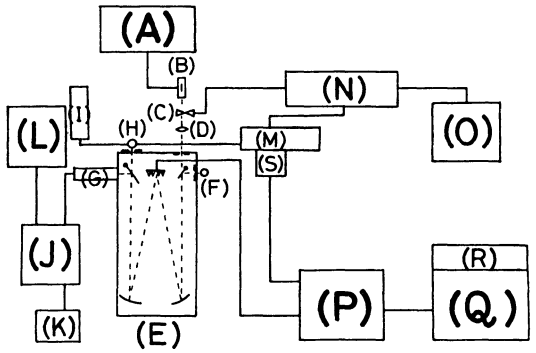

Fig. 1. Schematic diagram of computer-controlled instrumentation for multielement analysis.
(A) Flame gas controlls, (B) burner, (C) chopper, (D) lens, (E) monochromator, (F) Hg lamp, (G) SIT, (H) photomultiplier, (I) power supply, (J) optical multi-channel analyser, (K) oscilloscope, (L) X-Y recorder, (M) pre-amplifier, (N) lock-in-amplifier, (O) recorder, (P) minicomputer, (Q) teletype, (R) tape reader/puncher, (S) interface for peak sensor.

† Present address: Department of Chemistry, The University of Alberta, Edmonton, Alberta, Canada T6G 2G2.

†† N_2O, dinitrogen oxide in IUPAC nomenclature.

was selected by mirrors positioned beside the entrance and exit slits. The entrance slits were used to receive radiation from the flame and a mercury penray lamp, respectively, the latter being used for wavelength calibration of the monochromator scanning system. The flame focused on the entrance slit was imaged down a factor of 2 using a single spherical silica lens (diameter, 60 mm; focal length, 219 mm). The SIT detector tube (Princeton Applied Research Co., SIT 1205D/01) and a standard photomultiplier (Hamamatsu TV Co., R919) sensitive to ultraviolet and visible light were positioned at the exit ports. The slit unit was removed in the former case, and a plate was equipped on the SIT adaptor to obstruct 50% of the incident light to enable dark current correction. The lateral length of the SIT detector was 12.5 mm and for the monochromator RLD of 0.4 nm/mm, a 5 nm spectral window was obtained. The resolution power for the SIT, 0.032 nm, was about 7 times poorer than that by PMT (slit width, 10 μm). The SIT signal after processing in the OMA (Princeton Applied Research Co., OMA 1205A) was displayed on the oscilloscope and/or could be recorded by an external X-Y recorder (Yokogawa Electric Works, Ltd., 3078).

For PMT detection, a pre-amplifier (laboratory constructed), a light chopper and a lock-in-amplifier (Princeton Applied Research Co., 125A and 5203, respectively) were used.

A minicomputer (Hewlett Packard 2108) was employed to control the monochromator wavelength by the slew scanning technique. A mercury penray lamp (Ultra-Violet Co., 11SC-I) was used for initial wavelength calibration.

Procedure. For wavelength calibration, the scanning system was referenced to the mercury lines at 253.65 and 507.30 nm using the Hg lamp. This procedure determined the number of steps/wavelength (nm) to be employed in wavelength selection by the stepping motor, when controlling the grating angle. After calibration, the wavelengths of the desired atomic lines could be set arbitrarily by command from the computer. The details of the slew scanning system will be described elsewhere.[18]

The experimental conditions for the measurement of atomic emission using the nitrous oxide–acetylene flame were optimized in terms of the flame and slit conditions. Once the conditions had been optimized, a standard solution was aspirated and the accumulated spectrum was stored in OMA memory [A]. The procedure was repeated for the blank solution using memory [B]. The subtracted spectrum [A-B] provided the emission line(s) of the element(s). The emission intensity was obtained by noting the peak height (generally for channel 250±2) and subtracting the average reading of the side background for 10 channels around the peak channel. The background noise level ([A-B] spectrum for the channel range 240—260) was obtained when distilled water was aspirated and subtraction of the [A] and [B] memories was performed. The PMT detection system was used for comparison studies. The signal and background noise were measured from the pen deflection on the chart recorder paper.

The detection limits in Tables 1 and 2 are defined as the concentrations which represent a signal equivalent to twice the standard deviation of the background noise level. The values were obtained from the standard calibration curve for each element prepared by the least squares method. The optimized conditions determined are also summarized in Table 1 with the wavelengths of analytical lines. The chemicals used were of analytical reagent grade and deionized and distilled water was used as the blank solution.

Results and Discussion

Flame Background Correction. The atomic emission

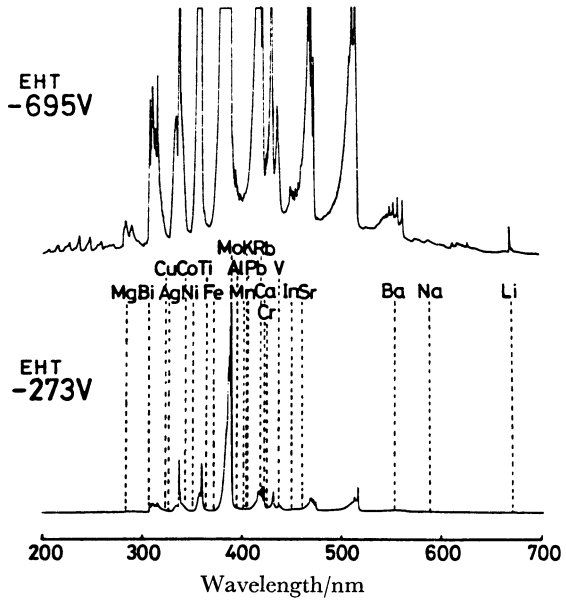

Fig. 2. Emission spectra of nitrous oxide–acetylene flame observed by photomultiplier tube.

of 22 elements in the nitrous oxide–acetylene flame was measured by the SIT–OMA system coupled to the programmable monochromator. Figure 2 shows the N_2O–C_2H_2 flame emission spectra recorded by the PMT when only distilled water was aspirated. The upper curve was recorded at a high EHT (−695 V) to indicate the prominent background constituents of the flame. Background species at approximate wavelengths are NO (200—280 nm), OH (280—330 nm), NH (336 nm), CN (350—442 nm), CH (387—431 nm), and C_2 (437—600 nm). The analytical lines of the elements used in the study are indicated by the dotted lines on the lower spectrum.

Flame emission spectra observed by the SIT–OMA system for a 5 nm spectral window are shown in Figs. 3

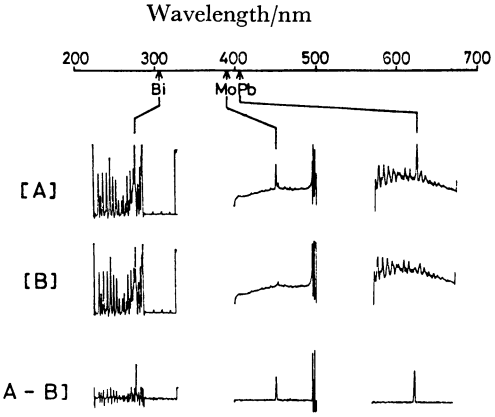

Fig. 3. Emission spectra observed by SIT–OMA system near Bi(306.8 nm), Mo(390.3 nm), and Pb(405.8 nm) lines in nitrous oxide–acetylene flame (Bi 100 μg/ml, Mo 10 μg/ml, Pb 50 μg/ml).
[A]: Spectra for sample solutions, [B]: spectra for blank solution, [A-B]: spectra corrected for flame background.

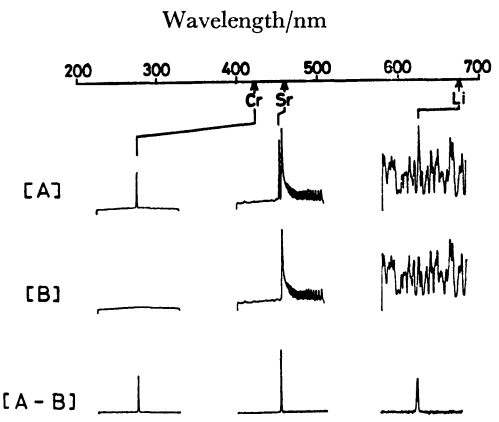

Fig. 4. Emission spectra observed by SIT–OMA system near Cr(425.4 nm), Sr(460.7 nm), and Li(670.8 nm) lines in nitrous oxide–acetylene flame (Cr 1 μg/ml, Sr 0.1 μg/ml, Li 0.005 μg/ml).
[A]: Spectra for sample solutions, [B]: spectra for blank solution, [A-B]: spectra corrected for flame background.

and 4 for Bi, Mo, Pb, and Cr, Sr, and Li, respectively. Since the SIT–OMS system has 2 memories, each memory was used for the emission measurements of the sample solution and the blank solution, respectively. Spectra [A-B] in Figs. 3 and 4 are the corrected spectra calculated from the [A] and [B] memories, and subtraction is automatically performed in the OMA. The background at the Bi wavelength is particularly severe and corresponds to the OH vibrational fine structure. The predominant background species at the Mo wavelength is CH, while at the Pb wavelength CN is predominant. For Sr and Li, the predominant species is C_2, while at the Cr wavelength flame background is negligible.

Detection Limits and Precision. The analytical performance data summarized in Table 1 were obtained by accumulating the signals for 4.1 s. In the SIT–OMA system, the scanning rate of the electron beam over 500 channels was 32.8 ms, and the 4.1 s accumulation time corresponded to 125 times accumulation of the signals at each channel in the SIT detector. The dynamic range of the SIT–OMA system is 10^5 counts and the real-time dynamic range (real-time is a single scan) is about 750 counts for each channel. Therefore, the entrance slit width and slit height were required to be adjusted to obtain the appropriate signal intensities which were within the dynamic range of the SIT–OMA system. Before adjustment of the slit conditions mentioned above, the flame conditions and height above the burner head were optimized for each element using a constant nitrous oxide flow rate of 7.5 l/min. The experimental results obtained through the above procedures are summarized in Table 1, along with the analytical lines and other experimental conditions. The detection limit data are similar to those obtained by Howell and Morrison[6] who used a 0.5 m monochromator–SIT combination. The relative standard deviation (RSD) values for the concentration indicated in parenthesis were generally in the 3% range, although for some elements of low sensitivity, *e.g.* Bi, Pb where concentrations were relatively closer to the respective detection limits, higher RSD values were obtained.

Regarding the flame operating conditions, it can be seen from Table 1 that the elements such as Ti, V, Al, and Mo were atomized effectively in the reducing atmosphere of the C_2H_2-rich flame and in the high temperature region corresponding to a high position above the burner head. These conditions are required to prevent formation of the refractory oxide species. In contrast, optimum sensitivity for Co, Pb, Fe was obtained in the oxygenated atmosphere of the C_2H_2-lean flame and at a low position above the burner. In this way, the optimum conditions in the N_2O–C_2H_2 flame are very different for the elements. This spread in the optimum values constitutes a major problem in utilizing the N_2O–C_2H_2 source for multielement analysis, since fixed flame conditions and flame height would be desirable for rapid analysis. The other major drawback in the N_2O–C_2H_2 excitation source is that elements whose resonance lines are in the UV region are not sufficiently excited to observe atomic emission.[19]

Comparison of SIT and PMT Detection. So far, to evaluate SIT detector performance, the detection limits obtained by the SIT image detector have been compared with those obtained in separate studies by the PMT.[1–10] In the present study, the detection limits of 8 elements were also obtained by a PMT (R919). The experimental conditions for the SIT detector were the same as those shown in Table 1, and the conditions for the PMT were independently determined by optimization procedures for each element.

As is well known,[6] the photon quantum yield of the SIT in the ultraviolet region is worse by 1—2 orders of magnitude when compared to that of the PMT, while it is almost comparable with or better than that of the PMT in the visible region. Although a rigorous comparison of data is ruled out due to fundamental design differences between the SIT and the PMT, for standard measurement conditions, *i.e.* SIT accumulation time of 4.1 s and a PMT time constant of 2 s, a general trend in the results can be pointed out. Poor SIT detector performance is evident in the UV, *e.g.* for Mg and Ag where detection limits are about 20 times poorer than the PMT data. The excellent detection power in the visible region is, however, clearly seen from Table 2.

Conclusions

Use of the SIT detector for slew scan multielement analysis is advantageous in that it allows for a less accurate wavelength setting of the monochromator than otherwise would be required for PMT detection. Rapid analysis may be performed with the present system (*e.g.*, less than 5 min required for 10 elements). The results shown in Tables 1 and 2 and Figs. 3 and 4 demonstrate the following important capabilities of the SIT–OMA system: 1) high detection limits for many elements, 2) multielement detection over a small wavelength range (5 nm), 3) the facility to correct for background interference. However, the relatively poor sensitivity of the SIT in the ultraviolet region and the insufficient excitation efficiency of the N_2O–C_2H_2 flame detract from the

Table 1. The flame emission detection limits of various elements for SIT detection under optimized experimental conditions

Element	Wavelength nm	C_2H_2[a] Flow rate l/min	Flame[b] height mm	Slit width μm	Slit height mm	Detection limit[c] μg/ml	RSD[d] %
Mg	285.21	5.75	7.5	70	3	0.22	3.0(1)
Bi	306.77	6.13	5	30	2.8	21	12.6(100)
Cu	324.75	5.75	4	165	2	0.066	5.6(1)
Ag	328.07	6.0	4	60	1	0.11	2.3(5)
Co	345.35	5.75	9	160	5	0.21	8.4(1)
Ni	352.45	5.75	6	150	3	0.61	2.8(10)
Ti	365.35	7.5	10	250	6	0.15	3.8(5)
Fe	371.99	5.75	8	150	5	0.13	7.2(1)
Mo	390.30	6.5	9	150	1	0.17	15.4(1)
Al	396.15	7.25	8	150	0.3	0.032	7.4(0.5)
Mn	403.08	6	5	100	1	0.017	2.1(1)
K	404.41	5.75	10	250	5	7.5	—
Pb	405.78	5.75	8	170	5	0.95	11.4(10)
Rb	420.19	5.75	6	150	1.4	2.2	5.1(50)
Ca	422.67	6	4.5	40	0.4	0.002	2.8(0.1)
Cr	425.43	6	6	120	1.5	0.0028	2.2(0.1)
V	437.92	7.5	8	125	2	0.018	2.4(0.5)
In	451.13	6	4.5	130	0.9	0.0092	1.6(0.5)
Sr	460.73	6.25	7	120	3	0.0008	1.5(0.05)
Ba	553.56	6.25	4.5	180	1	0.064	3.7(1)
Na	589.00	6	7.5	100	1.5	0.00066	—
Li	670.78	6.25	6	170	2.3	0.00013	2.1(0.005)

a) The flow rate of nitrous oxide was fixed at 7.5 l/min. b) Height above the burner head. c) See text for definition. d) Relative standard deviation calculated from 10 determinations. Value in parenthesis is concentration at which determination was performed.

Table 2. Comparison of detection limits for SIT and PMT

Element	Wavelength nm	SIT μg/ml	PMT μg/ml
Mg	285.21	0.24	0.004
Bi	306.77	24	23
Ag	328.07	0.20	0.060
Mo	390.30	0.39	0.87
Pb	405.78	0.35	0.48
Cr	425.44	0.005	0.018
Sr	460.73	0.0005	0.0007
Li	670.78	0.00028	0.0022

use of the present instrumental system for analytical flame emission spectrometry. Particularly, the flame requires tedious optimization procedures to achieve sufficient sensitivity for each element. The ICP excitation system would overcome to some extent the poor SIT sensitivity in the UV. A further advantage of the ICP source relative to the N_2O–C_2H_2 flame is that near-optimum sensitivity for all elements is provided by one set of ICP operating conditions.[20] The application of the present instrumental system to ICP emission spectrometry is in progress, and will be reported in the near future[21].

The authors express their thanks to Dr. A. Otsuki, National Institute for Environmental Studies, for his helpful discussion and encouragement. C.W.M. is grateful to the Inner London Education Authority (U.K.) for the award of The Robert Blair Fellowship and receipt of a travel grant.

References

1) K. W. Busch, N. G. Howell, and G. H. Morrison, *Anal. Chem.*, **46**, 575, 1231 (1974).
2) F. L. Fricke, O. Rose, Jr., and J. A. Caruso, *Anal. Chem.*, **47**, 2018 (1975).
3) F. L. Fricke, O. Rose, Jr., and J. A. Caruso, *Talanta*, **23**, 317 (1976).
4) N. G. Howell, J. D. Ganjei, and G. H. Morrison, *Anal. Chem.*, **48**, 319 (1976).
5) J. D. Ganjei, N. G. Howell, J. R. Roth, and G. H. Morrison, *Anal. Chem.*, **48**, 505 (1976).
6) N. G. Howell and G. H. Morrison, *Anal. Chem.*, **49**, 106 (1977).
7) D. G. Mitchell, K. W. Jackson, and K. M. Aldous, *Anal. Chem.*, **45**, 1215A (1973).
8) K. W. Jackson, K. M. Aldous, and D. G. Mitchell, *Appl. Spectrosc.*, **28**, 569 (1974).
9) K. M. Aldous, D. G. Mitchell, and K. W. Jackson, *Anal. Chem.*, **41**, 1034 (1975).
10) T. L. Chester, H. Haraguchi, D. O. Knapp, J. D. Messman, and J. D. Winefordner, *Appl. Spectrosc.*, **30**, 410 (1976).
11) Y. Talmi, *Anal. Chem.*, **47**, 658A, 699A (1975).
12) E. Cordos and H. V. Malmstadt, *Anal. Chem.*, **45**, 425 (1973).
13) D. J. Johnson, F. W. Plankey, and J. D. Winefordner, *Anal. Chem.*, **47**, 1739 (1975).
14) R. W. Spillman and H. V. Malmstadt, *Anal. Chem.*, **48**, 303 (1976).

15) P. W. J. M. Boumans, G. H. van Gool, and J. A. J. Jansen, *Analyst*, **101**, 585 (1976).
16) H. Kawaguchi, M. Okada, T. Ito, and A. Mizuike, *Anal. Chim. Acta*, **95**, 145 (1977).
17) V. A. Fassel, *Science*, **202**, 183 (1978).
18) N. Furuta, H. Haraguchi, and K. Fuwa, *Anal. Chem.*, to be submitted.
19) G. D. Christian, and F. J. Feldman, *Appl. Spectrosc.*, **25**, 660 (1971).
20) R. H. Scott, V. A. Fassel, R. N. Kniseley, and D. E. Nixon, *Anal. Chem.*, **46**, 75 (1974).
21) N. Furuta, C. W. McLeod, H. Haraguchi, and K. Fuwa, *Appl. Spectrosc.*, to be submitted.